Ceramics International 45 (2019) 5553–5558

Contents lists available at ScienceDirect

Ceramics International

journal homepage: www.elsevier.com/locate/ceramint

Thermoelectric properties and stability of the $Re_{0.2}Sr_{0.8}CoO_{3-\delta}$ Re = Gd, Dy) complex cobalt oxides in the temperature range of 300–800 K

V.A. Dudnikov[a], Yu.S. Orlov[a,b,*], N.V. Kazak[a], A.S. Fedorov[a,b], L.A. Solov'yov[c], S.N. Vereshchagin[c], A.T. Burkov[d], S.V. Novikov[d], S.G. Ovchinnikov[a,b]

[a] Kirensky Institute of Physics, Federal Research Center "Krasnoyarsk Scientific Center, Russian Academy of Sciences, Siberian Branch", Krasnoyarsk 660036 Russia
[b] Siberian Federal University, Institute of Engineering Physics and Radio Electronics, Krasnoyarsk 660041 Russia
[c] Institute of Chemistry and Chemical Technology, Federal Research Center "Krasnoyarsk Scientific Center, Russian Academy of Sciences, Siberian Branch", Krasnoyarsk 660036 Russia
[d] Ioffe Physicotechnical Institute, Russian Academy of Sciences, St. Petersburg 194021 Russia

ARTICLE INFO

Keywords:
Substituted rare earth cobalt oxides
Thermoelectric oxide materials
Ordered and disordered states

ABSTRACT

Temperature dependences of the electrical resistivity and Seebeck coefficient of the $Re_{0.2}Sr_{0.8}CoO_{3-\delta}$ Re = Gd, Dy) complex cobalt oxides in the temperature range of 300 – 800 K have been investigated. The effects of ordering in the cation and anion sublattices on the thermoelectric properties has been examined and their comparative analysis has been made. It was found that, in the investigated temperature range, the thermoelectric power factor of the ordered compounds significantly exceeds the analogous parameter of the disordered samples. The temperature dependence of the electrical resistivity was shown to obey the activation law. As the temperature increases, the samples undergo a semiconductor-semiconductor electronic transition with a decrease in the activation energy. The thermoelectric properties of all the samples are shown to be stable in the investigated temperature range. The maximum thermoelectric power factor of the ordered $Dy_{0.2}Sr_{0.8}CoO_{2.67}$ cobaltite at a temperature of 360 K has been obtained; it amounts to 0.23 μW/(cm·K^2), which is a good parameter for this class of materials.

1. Introduction

The main characteristic of the properties, quality, and application efficiency of a thermoelectric material is the thermoelectric efficiency $Z = S^2\sigma/\varkappa$ (S is the Seebeck coefficient (also known as thermopower), σ is the electrical conductivity, and $\varkappa$ is the thermal conductivity) with the reciprocal temperature dimensionality [1]. The most commonly used dimensionless parameter is the thermoelectric Q factor $ZT = (S^2\sigma T/\varkappa)$ (T is the absolute temperature), which determines the efficiency of a thermoelectric converter or the refrigeration efficiency of a thermoelectric cooler and makes it convenient to compare different thermoelectric materials.

Another important parameter is the power factor $P = S^2\sigma$ determined by the electronic properties of a material, including thermopower S and electrical conductivity σ. If the specific power of energy conversion is more important than the efficiency, the high power factor is of greater importance for application than the thermoelectric conversion efficiency Z.

Recently, much attention has been paid to oxide materials [2], since they are stable against high temperatures, nontoxic and, as a rule, contain no rare elements. Among the oxides promising for application are several groups of cobaltites, including $Bi_2Sr_2Co_2O_y$ whiskers ($S \approx 300$ μV/K at 973 K, $ZT > 1.1$) [3,4], layered $Na_xCo_2O_4$ [5], misfit-layered $[M_xA_2O_{x+2}]_y[CoO_2]$ (M = Co, Bi, Tl; A = Ca, Sr, Ba; m = 0, 1, 2; $y \geq 0.5$) [6,7] cobalt-oxide systems, and $Ln_{1-x}A_xCo_{1-y}M_yO_{3-\delta}$ (Ln is the lanthanide, A is the alkali or alkaline earth metal, and M is the transition metal) compounds with a perovskite-like structure [8–13]. As strongly correlated electron systems, the $Ln_{1-x}A_xCo_{1-y}M_yO_{3-\delta}$ compounds also of great interest for fundamental research [14]. The rare-earth cobalt oxides are characterized by the competition of the Co^{3+} ion spin states, which leads to the orbital and magnetic ordering and affects the magnetic, electrical, and structural properties of the materials [15–19].

During the $Ln_{1-x}Sr_xCoO_{3-\delta}$ perovskites formation, different equilibrium distributions of Sr^{2+} and Ln^{3+} ions can be established, depending on the ratio between ionic radii of the cations. For the Ln = {La–Nd} elements, the structure with a completely disordered distribution of Sr^{2+}/Ln^{3+} cations over the A sites of the ABO_3 perovskite

* Correspondence to: Kirensky Institute of Physics KSC SB RAS, 660036 Krasnoyarsk, Russia.
E-mail addresses: jso.krasn@mail.ru, orlov@iph.krasn.ru (Y.S. Orlov).

https://doi.org/10.1016/j.ceramint.2018.12.013
Received 11 October 2018; Received in revised form 30 November 2018; Accepted 3 December 2018
Available online 04 December 2018

structure is stable at all temperatures. If the substitute radius is smaller than the Nd^{3+} ion radius, the disordered perovskites exist at high temperatures; in the low-temperature region, the structure with the ordered Sr^{2+} and Ln^{3+} cations and anionic vacancies is stable [20]. The disordered $Ln_{1-x}Sr_xCoO_{3-\delta}$ perovskites can be obtained in the form of metastable phases by quenching the high-temperature states [21]. We synthesized the ordered and disordered $Re_{0.2}Sr_{0.8}CoO_{3-\delta}$ Re = Gd, Dy) polycrystalline samples and studied the behavior of the electrical resistivity and Seebeck coefficient of the $Re_{0.2}Sr_{0.8}CoO_{3-\delta}$ Re = Gd, Dy) complex cobalt oxides in the temperature range of 300–800 K.

2. Experimental methods

2.1. Synthesis

To obtain the $Re_{0.2}Sr_{0.8}CoO_{3-\delta}$ Re = Gd, Dy) polycrystalline samples ordered (ReSC-ord) and disordered (ReSC-dis) over the A sites of the perovskite crystal structure, we used a standard ceramic technology with multiple sintering and grinding of the annealed charge consisting of the Gd_2O_3 and Co_3O_4 oxides and strontium carbonate $SrCO_3$ [21,22]. No additional annealing at 773 K for oxygen saturation of the samples [23] was performed.

The oxygen non-stoichiometry was determined on a NETZSCH-STA449C analyzer equipped with an Aeolos QMS 403 C mass spectrometer. The measurements were performed in the 5% H_2-Armixture flow in a corundum crucible with a perforated cover (the sample mass was 22 ± 0.5 mg). The oxygen content in the $Gd_{0.2}Sr_{0.8}CoO_{3-\delta}$ and $Dy_{0.2}Sr_{0.8}CoO_{3-\delta}$ samples was determined from a decrease in the sample mass upon reduction, similarly to the procedure described in [24] using the technique from [25].

The X-ray diffraction study was carried out on a PANalyticalX'Pert PRO powder diffractometer (Netherlands, CoKα) in the 2θ angular range of 10–120°. The crystal lattice parameters were determined from the positions of diffraction maxima [26]; the crystal structure was refined using the X-ray diffraction pattern full profile by the Rietveld technique [27] and Derivative Difference Minimization (DDM) method [28].

The temperature dependences of the Seebeck coefficient and electrical resistivity were obtained on an experimental setup for thermopower and resistivity measurements [29] at the Ioffe Physicotechnical Institute, Russian Academy of Sciences.

3. Results and discussion

The formation of ordered/disordered structures depends on the rate of cooling from a synthesis temperature of T_s = 1473 K. Upon slow cooling from T_s at a rate of up to 2 deg/min, a cation-ordered ReSC-ord Re = Gd, Dy) perovskite structure forms; if the cooling rate exceeds 30 deg/s (quenching), a disordered ReSC-dis structure is obtained.

The disordered ReSC-dis structure represents a cubic perovskite phase with a random uniform distribution of Sr^{2+}/Re^{3+} ions over the crystal lattice with the formation of a metastable single-phase material with the cubic structure. The ordered ReSC-ord structures are characterized by the formation of a low-symmetry phase due to the partial ordering of Sr^{2+}/Re^{3+} cations and anionic vacancies, which can be observed as additional superstructural reflections in the X-ray diffraction patterns. Typical ReSC-dis and ReSC-ord Re = Gd, Dy) X-ray diffraction patterns are shown in Fig. 1 and Fig. S1 of the Supplementary Materials.

According to the determined oxygen non-stoichiometry index, we may assume the oxygen deficiency to be the same in the samples with the same ordering within the measurement error. The main properties of the samples are given in Table 1.

The electrical resistivity and thermopower were measured on the samples in the form of rectangular parallelepipeds (1–2) x 5 x (13–15) mm in size in the temperature ranges of 300–700 K for $Gd_{0.2}Sr_{0.8}CoO_{3-\delta}$ and 300–800 K for $Dy_{0.2}Sr_{0.8}CoO_{3-\delta}$ in the inert atmosphere (He, 99.999%). To study the stability of the samples in the high-temperature region, the measurements were performed during the heating-cooling cycles and the temperature dependences were compared. None of the investigated samples showed significant discrepancies between the temperature dependences of the electrical resistivity and thermopower in the heating-cooling cycle, which is indicative of their high stability. The dependences qualitatively correspond to the semiconductor conductivity type $d\rho/dT < 0$ over the entire temperature range (Fig. 2).

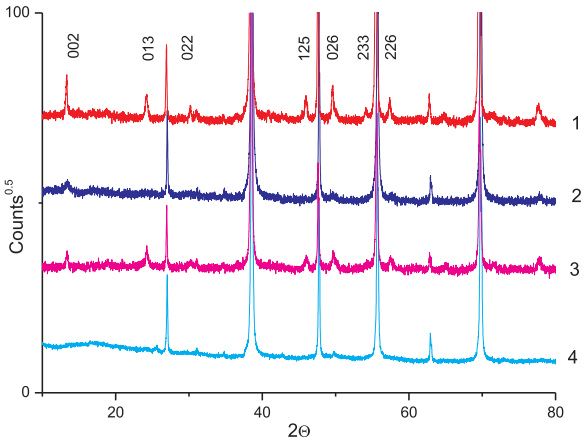

Fig. 1. X-ray diffraction patterns of the $Re_{0.2}Sr_{0.8}CoO_{3-\delta}$ samples. Superstructural reflexions of the tetragonal perovskite are denoted by indices: (1) $Gd_{0.2}Sr_{0.8}CoO_{3-\delta}$ (GSC-ord), (2) $Gd_{0.2}Sr_{0.8}CoO_{3-\delta}$ (GSC-dis), (3) $Dy_{0.2}Sr_{0.8}CoO_{3-\delta}$ (DSC-ord), and (4) $Dy_{0.2}Sr_{0.8}CoO_{3-\delta}$ (DSC-dis).

The electrical resistivity values for the $Gd_{0.2}Sr_{0.8}CoO_{3-\delta}$ and $Dy_{0.2}Sr_{0.8}CoO_{3-\delta}$ samples with the Re^{3+}/Sr^{2+} ions and oxygen vacancies ordered over the A sites are significantly different from the parameter of the samples with a random uniform distribution of the Re^{3+}/Sr^{2+} ions. Because of the absence of additional annealing at 773 K, the oxygen content in the disordered samples is much lower than in the ordered samples and the oxygen non-stoichiometry index δ of the GSC-dis samples (δ = 0.42) significantly exceeds a value of δ = 0.29 obtained in our previous work [24]. This also explains the discrepancy between the resistivities for GSC-dis at T = 300 K ρ = 40 mΩ/cm in [24] and ρ = 840 mΩ/cm obtained in this study. Due to the lower oxygen mobility in the ReSC-ord samples [21,30], additional annealing in air at 773 K does not affect the δ value.

The temperature dependences of the electrical resistivity demonstrate that the electrical resistivity of the GSC-dis rapidly decreases with increasing temperature and, around T = 600 K, becomes lower than the value for GSC-ord (Fig. 2a), while the DSC-dis resistivity is significantly higher than that of the DSC-ord samples over the entire temperature range (Fig. 2b).

According to the results of the earlier studies on the low-temperature electrical resistivity of substituted cobaltites, the conductivity mechanism changes from variable range hopping (VRH) for thermoactivation with increasing temperature [24]. Fig. 3 shows reciprocal temperature dependences of the resistivity logarithm for the samples at high temperatures. For all the samples, the $\ln \rho(1/T)$ curves contain the portions $300 < T < 400$ K (portion HT1) and $500 < T < 800$ K (portion HT2), which are described well by the linear dependence $\rho(T) = \rho_0 \cdot \exp(E_a/k_B T)$, where ρ_0 is the coefficient weakly dependent on temperature, E_a is the activation energy, k_B is the Boltzmann constant. As the temperature increases, the activation energy lowers. Thus, the E_a value for the GSC-dis and DSC-dis compositions in portion HT2 is twice as small as in portion HT1, while for the GSC-ord and DSC-ord samples, the E_a value decreases by an order of magnitude (Table 2). In the intermediate temperature range, the $\ln \rho(1/T)$ curves demonstrate the change in the slope angle, which is indicative of the change in the E_a value. These changes can be clearer seen in the temperature

Table 1
Structure and oxygen non-stoichiometry index δ for the $Re_{0.2}Sr_{0.8}CoO_{3-\delta}$ Re = Gd, Dy) samples at room temperature.

Sample	δ	State	Lattice	a, Å	b, Å	c, Å
$Gd_{0.2}Sr_{0.8}CoO_{3-\delta}$	0.42 ± 0.01	disordered	cubical	3.8342 (6)		
$Gd_{0.2}Sr_{0.8}CoO_{3-\delta}$	0.37 ± 0.01	ordered	tetragonal	7.6785(2)		15.3981 (5)
$Dy_{0.2}Sr_{0.8}CoO_{3-\delta}$	0.43 ± 0.01	disordered	cubical	3.8355		
$Dy_{0.2}Sr_{0.8}CoO_{3-\delta}$	0.37 ± 0.01	ordered	tetragonal	7.6754		15.365

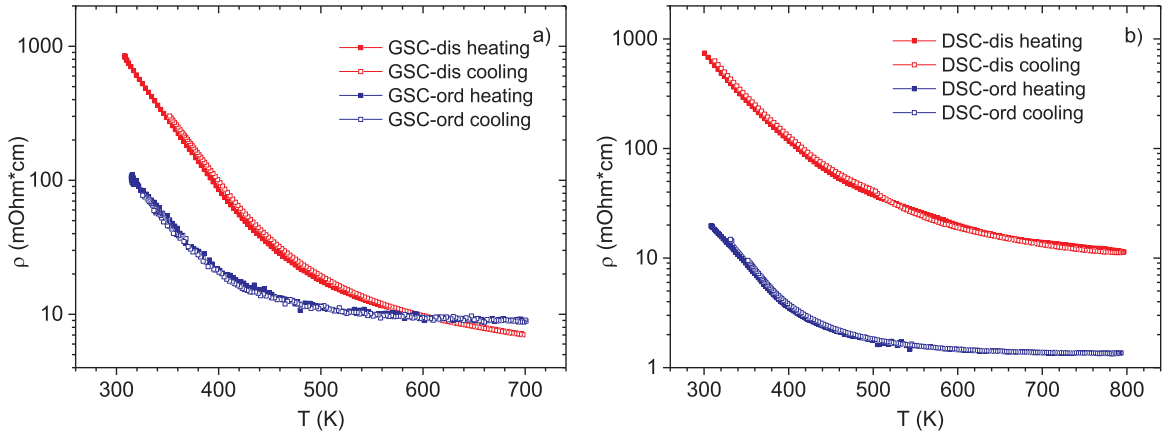

Fig. 2. Temperature dependences of the resistivity for (a) the $Gd_{0.2}Sr_{0.8}CoO_{3-\delta}$ and (b) $Dy_{0.2}Sr_{0.8}CoO_{3-\delta}$ compounds upon heating and cooling.

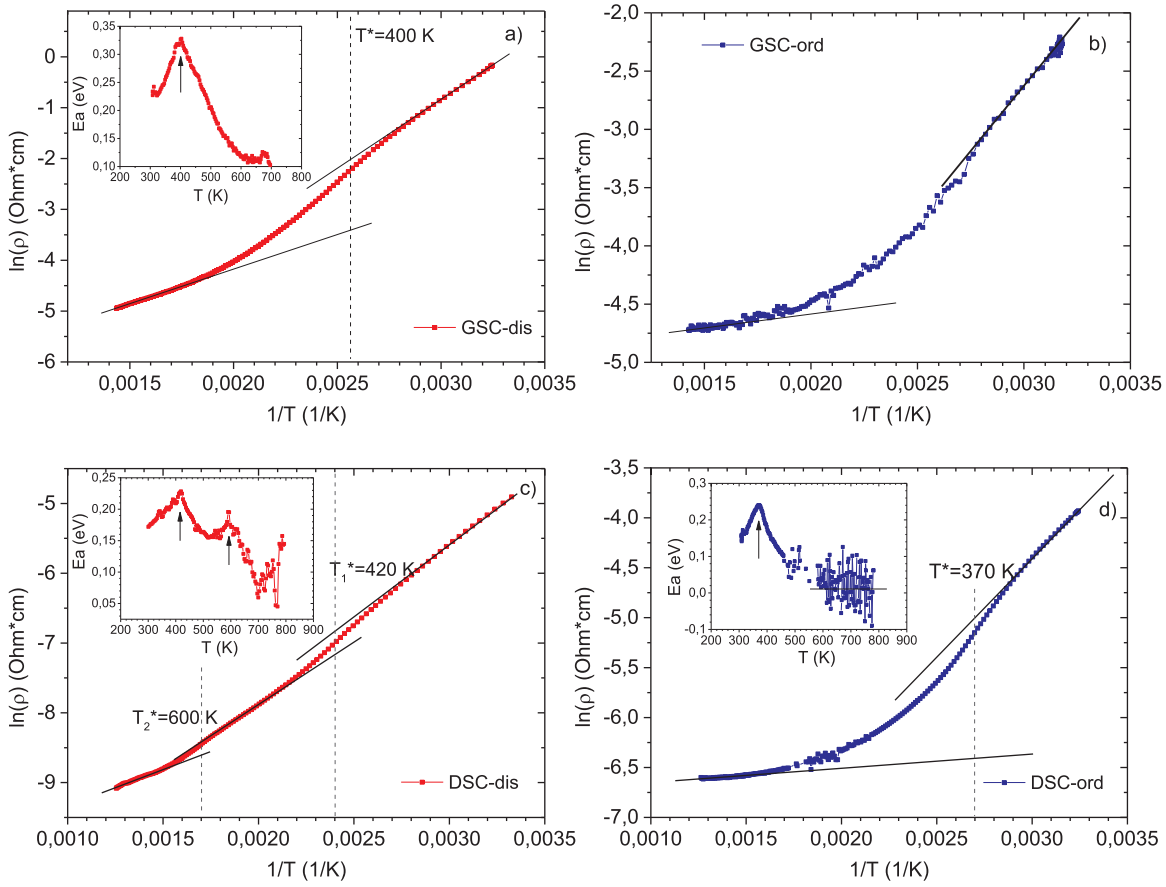

Fig. 3. Reciprocal temperature dependences of the resistivity logarithm for (a, b) the ordered and disordered $Gd_{0.2}Sr_{0.8}CoO_{3-y}$ and (c, d) $Dy_{0.2}Sr_{0.8}CoO_{3-y}$ compounds. Black straights show the thermo-activation law processing. Insets: temperature dependences of the activation energy. The temperatures of the electronic transitions are shown by arrows and dashed lines.

Table 2
Parameters of thermoactivation conductivity and temperature of the electronic transitions in the $Re_{0.2}Sr_{0.8}CoO_{3-\delta}$ Re = Gd, Dy) cobaltites.

	HT1 (T < 400 K)		HT2 (T > 500 K)	
	$\rho_0 0.10^{-3}$ (Ω cm)	E_a (eV)	$\rho_0 0.10^{-3}$ (Ω cm)	E_a (eV)
GSC-dis	0.117 ± 0.003	0.236 ± 0.001	1.059 ± 0.004	0.114 ± 0.001
GSC-ord	0.095 ± 0.010	0.190 ± 0.003	6.026 ± 0.289	0.024 ± 0.003
DSC-dis	0.678 ± 0.026	0.181 ± 0.001	3.006 ± 0.067	0.092 ± 0.001
DSC-ord	0.036 ± 0.001	0.168 ± 0.001	1.086 ± 0.009	0.014 ± 0.001

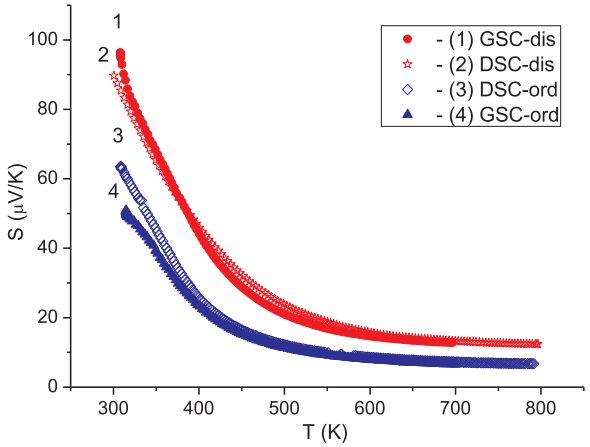

Fig. 4. Temperature dependences of the Seebeck coefficient for (1) the $Gd_{0.2}Sr_{0.8}CoO_{3-\delta}$ (GSC-dis), (2) $Dy_{0.2}Sr_{0.8}CoO_{3-\delta}$ (DSC-dis), (3) $Dy_{0.2}Sr_{0.8}CoO_{3-\delta}$ (DSC-ord), and (4) $Gd_{0.2}Sr_{0.8}CoO_{3-\delta}$ (GSC-ord) samples.

dependence of the activation energy determined from the first derivative $E_a(T) = d(\ln \rho(T))/d(1/T)$ and shown in the insets in the corresponding figures. It can be seen that the activation energy of the samples sharply increases near the critical temperature T^*. An exception is the GSC-ord sample, for which such an analysis cannot be made because of the noisy electrical resistivity data. The behavior of electrical resistivity and resulting temperature dependences of the activation energy show that the investigated cobaltites undergo semiconductor-semiconductor electronic transitions. The determined critical temperatures are similar to the temperatures corresponding to a sharp decrease in the Seebeck coefficient and maxima in the temperature dependences of the power factor.

The measured Seebeck coefficients S are shown in Fig. 4. For all the samples, the thermopower monotonically decreases with increasing temperature. The $S(T)$ temperature dependences of the disordered $Re_{0.2}Sr_{0.8}CoO_{3-\delta}$ Re = Gd, Dy) samples at temperatures above 350 K are identical and almost coincide in magnitude. The similar situation is

Table 3
Maximum thermoelectric power factors and corresponding temperatures.

Sample	State	P_{max} (μW/(cm K^2))	T_{max} (K)
$Gd_{0.2}Sr_{0.8}CoO_{2.58}$	disordered	0.026	460
$Gd_{0.2}Sr_{0.8}CoO_{2.67}$	ordered	0.03	370
$Dy_{0.2}Sr_{0.8}CoO_{2.57}$	disordered	0.019	425
$Dy_{0.2}Sr_{0.8}CoO_{2.67}$	ordered	0.23	360

observed in the GSC-ord and DSC-ord samples above 400 K. The absolute values of S for the ReSC-dis sample exceed the S values of the ReSC-ord sample over the entire temperature range.

Fig. 5a and b show temperature dependences of the power factor P. It can be seen that, as the temperature increases, the power factor of all the samples first grows, attaining its maximum, and then decreases. The ordered $Gd_{0.2}Sr_{0.8}CoO_{3-\delta}$ and $Dy_{0.2}Sr_{0.8}CoO_{3-\delta}$ compounds are characterized by a monotonic decrease; the disordered samples have minima around 600 K with the subsequent increase. The ordering of Sr^{2+}/Re^{3+} cations and anionic vacancies leads to an increase in the maximum power factor and shift of the maxima in the temperature dependences to the low-temperature region (Table 3).

In the case of the disordered samples, the absence of stabilizing annealing at T = 773 K leads to higher oxygen non-stoichiometry δ and decrease of mobile weakly bound oxygen amounts in the $Gd_{0.2}Sr_{0.8}CoO_{3-\delta}$ lattice. In the case of ordered samples, the influence of stabilization annealing on the δ value was not observed.

In Fig. 6 the resistivity ρ, the Seebeck coefficient S and power factors temperature dependencies are compared for stabilized (temperature range up to 300 K) [26] and unstabilized $Gd_{0.2}Sr_{0.8}CoO_{3-\delta}$ samples (temperature above 300 K). As could be seen from the figures, the increase in δ radically changes the value of the electrical resistivity of the disordered samples, while at the same time the changes in thermopower values are insignificant.

It should be noted that the stabilization of the high-temperature properties of the disordered samples in an inert atmosphere is achieved by minimizing the amount of weakly bound oxygen in the lattice. Thus, it is possible to divide the thermoelectric properties into high-

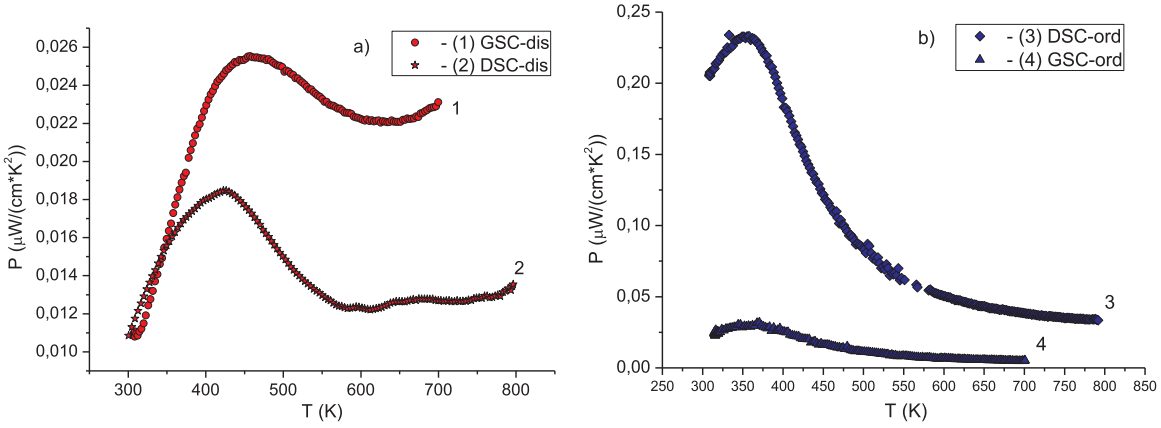

Fig. 5. Temperature dependences of the power factor P for (a) the disordered and (b) ordered samples.

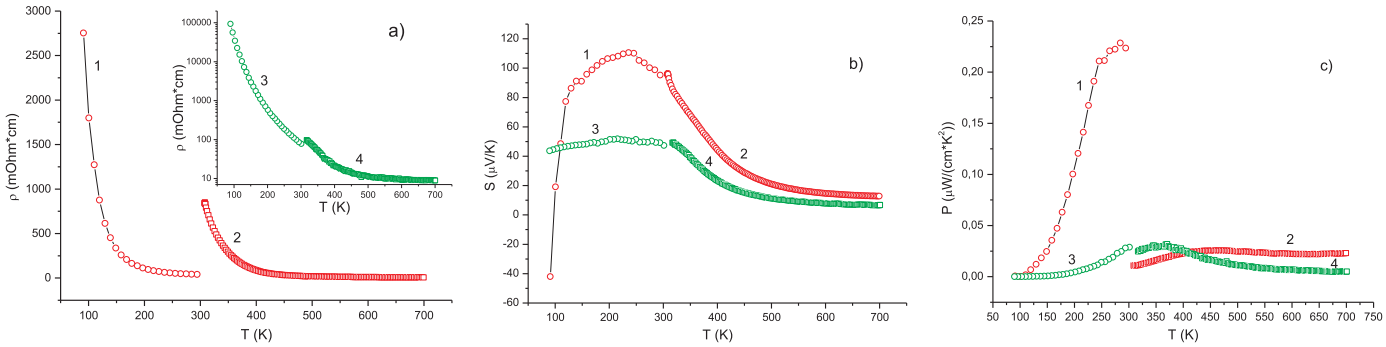

Fig. 6. Temperature dependencies of electrical resistivity (a), thermopower (b) and power factor (c) of ordered and unordered samples of $Gd_{0.2}Sr_{0.8}CoO_{3-\delta}$. The temperature range below 300 K corresponds to the oxygen-stabilized samples, temperatures above 300 K – without stabilization. (1), (2) are disordered samples with $\delta = 0.29$ and $\delta = 0.42$, correspondingly; (3), (4) are ordered with $\delta = 0.37$.

temperature ($T > 300$ K) and low-temperature ($T < 300$). In the low-temperature region, the presence of weakly bound oxygen in disordered $Gd_{0.2}Sr_{0.8}CoO_{3-\delta}$ leads to a decrease in electrical resistance and 9 times increase in the power factor P at $T = 300$ K. In the high-temperature region, after the amount of mobile oxygen is minimized, the situation changes. The best thermoelectric properties are shown by the ordered samples, which is observed in $Dy_{0.2}Sr_{0.8}CoO_{3-\delta}$ compounds (Fig. 5b) for which the value of P is 10 times more at $T = 350$ K than for the disordered compounds.

The power factors obtained in this work for the sample $Dy_{0.2}Sr_{0.8}CoO_{2.67}$ with cations and anionic vacancies ordered over the A sites ($P = 0.23$ μW/(cm·K^2)) are consistent with those presented in study [31] for the $LaCo_{1-x}Ni_xO_3$ ($P = 0{,}12$ μW/(cm·K^2)), $LaCo_{1-x}Ti_xO_{3-\delta}$ ($P = 0.28$ μW/(cm·K^2)) [32], $La_{1-x}Sr_xCo_{0.8}Ni_{0.1}Fe_{0.1}O_3$ ($P = 0.76$ μW/(cm·K^2)) [33], and $La_{1-x}Na_xCoO_3$ ($P = 0.1$ μW/(cm·K^2)) polycrystalline samples [34], although our data are inferior to the value of $P \approx 3$ μW/(cm·K^2) for the $Ca_{3-x}Bi_xCo_4O_{9+\delta}$ samples from study [35].

4. Conclusions

In our previous study [24], we investigated the low-temperature thermoelectric properties of the $Gd_{0.2}Sr_{0.8}CoO_{3-\delta}$ solid solutions. The electrical resistivity and heat conductivity of the disordered compositions were lower than those of the ordered ones and the Seebeck coefficient, on the contrary, was higher. This led to the much higher thermoelectric efficiency of the disordered samples (the maximum values obtained were $ZT = 0.057$ for the $Gd_{0.2}Sr_{0.8}CoO_{2.71}$-dis compound at $T = 284$ K and $ZT = 0.002$ for the $Gd_{0.2}Sr_{0.8}CoO_{2.63}$-ord compound at $T = 300$ K; the power factors were $P = 0.22$ μW/(cm·K^2) and $P = 0.03$ μW/(cm·K^2), respectively). An increase in the oxygen non-stoichiometry of the disordered samples from $\delta = 0.29$ to $\delta = 0.42$ resulted in the significant growth of the electrical resistivity, which affected the Seebeck coefficient and power factor discussed in this work ($\rho = 40$ mΩ/cm, $S = 87.5$ μV/K, $P = 0.19$ μW/(cm K^2) for $\delta = 0.29$ and $\rho = 840$ mΩ/cm, $S = 96$ μV/K, $P = 0.01$ μW/(cm·K^2) for $\delta = 0.42$ at $T = 300$ K).

In the low-temperature region, the presence of weakly bound oxygen in the disordered $Gd_{0.2}Sr_{0.8}CoO_{3-\delta}$ samples enhances the P value by a factor of 9 at $T = 300$ K as compared with the ordered samples. These differences show that the thermoelectric parameters of these compounds are significantly affected not only by the degree of ordering of the cations and anionic vacancies over the A sites of the perovskite structure, but also by the amount of mobile oxygen in the disordered samples. In the high-temperature region, on the contrary, the ordered samples exhibit the best thermoelectric properties, which is observed in the $Dy_{0.2}Sr_{0.8}CoO_{3-\delta}$ samples (Fig. 5b) characterized by the P value greater than that of the disordered samples by an order of magnitude. Thus, the strict control of the mobile oxygen amount δ in the disordered samples will make it possible to considerably improve the power factor P of this class of compounds.

In all the samples, we observed the thermoactivation conductivity type and occurrence of a semiconductor-semiconductor electronic transition extended in temperature and accompanied by a decrease in the activation energy. The consistency of the temperature dependences of the electrical resistivity and Seebeck coefficient upon heating and cooling in the investigated temperature range confirms the high stability of the complex ceramic cobalt oxides.

The maximum thermoelectric power factor was obtained for the disordered $Dy_{0.2}Sr_{0.8}CoO_{2.67}$ cobaltite at a temperature of 360 K. It was found to be 0.23 μW/(cm K^2), which is currently a good parameter for this class of materials confirming the expediency of further search for new promising compounds in the series of complex transition metal oxides.

Acknowledgements

This study was supported by the Russian Science Foundation, project no. 16-13-00060, Russia.

Appendix A. Supplementary material

Supplementary data associated with this article can be found in the online version at doi:10.1016/j.ceramint.2018.12.013.

References

[1] (a) A.F. Ioffe, Semiconductor Thermoelements and Thermoelectric Cooling, Infosearch, London, 1957;
(b) D.W. Rowe, CRC Handbook of Thermoelectrics, CRC Press, 1995.
[2] X. Shiand, L. Chenand, C. Uher, Recent advances in high-performance bulk thermoelectric materials, Int. Mater. Rev. 61 (2016) 379–415.
[3] R. Funahashi, M. Shikano, $Bi_2Sr_2Co_2Oy$ whiskers with high thermoelectric figure of merit, Appl. Phys. Lett. 81 (2002) 1459–1461.
[4] H.C. Hsu, W.L. Lee, K.K. Wu, Y.K. Kuo, B.H. Chen, F.C. Chou, Enhanced thermoelectric figure-of-merit ***ZT*** for hole-doped $Bi_2Sr_2Co_2O_y$ through Pb substitution, J. Appl. Phys. 111 (2012) 103709 (1–5).
[5] I. Terasaki, Y. Sasago, K. Uchinokura, Large thermoelectric power in $NaCo_2O_4$ single crystals, Phys. Rev. B: Condens. Matter 56 (1997) R12685–R12687.
[6] D. Moser, L. Karvonen, S. Populoh, M. Trottmann, A. Weidenkaff, Influence of the oxygen content on thermoelectric properties of $Ca_{3-x}Bi_xCo_4O_{9+\delta}$ system, Solid State Sci. 13 (2011) 2160–2164.
[7] H. Yamauchi, L. Karvonen, T. Egashira, Y. Tanaka, M. Karppinen, Ca-for-Sr substitution in the thermoelectric $[(Sr,Ca)_2(O,OH)_2]q[CoO_2]$, J. Solid State Chem. 184 (2011) 64–69.
[8] R. Robert, M.H. Aguirre, P. Hug, A. Reller, A. Weidenkaff, High-temperature thermoelectric properties of Ln(Co, Ni)O3 (Ln = La, Pr, Nd, Sm, Gd and Dy) compounds, Acta Mater. 55 (2007) 4965–4972.
[9] H. Hashimoto, T. Kusunose, T. Sekino, Influence of ionic sizes of rare earths on thermoelectric properties of perovskite-type rare earth cobalt oxides $RCoO_3$ (R = Pr, Nd, Tb, Dy), J. Alloy. Compd. 484 (2009) 246–248.
[10] H. Hashimoto, T. Kusunose, T. Sekino, thermoelectric properties of perovskite-type rare earth cobalt oxide solid solutions $Pr_{1-x}Dy_xCoO_3$, J. Ceram. Process. Res. 12 (3) (2011) 223–227.
[11] A. Weidenkaff, M.H. Aguirre, L. Bocher, M. Trottmann, P. Tomes, R. Robert,

Development of perovskite-type cobaltates and manganates for thermoelectric oxide modules, J. Korean Ceram. Soc. 47 (1) (2010) 47–53.
[12] S.G. Harizanova, E.N. Zhecheva, V.D. Valchev, M.G. Khristova, R.K. Stoyanova, Improving the thermoelectric efficiency of Co based ceramics, Mater. Today.: Proc. 2 (2015) 4256–4261.
[13] T. Wu, P. Gao, Development of perovskite-type materials for thermoelectric application, Materials 11 (2018) 999 (1–32).
[14] N.B. Ivanova, S.G. Ovchinnikov, M.M. Korshunov, I.M. Eremin, N.V. Kazak, Specific features of spin, charge, and orbital ordering in cobaltites, Phys.-Uspekhi 52 (2009) 789–810.
[15] N.A. Babushkina, A.N. Taldenkov, S.V. Strelsov, A.V. Kalinov, T.G. Kuzmova, A.A. Kamenev, A.R. Kaul, D.I. Khomskii, K.I. Kugel, Effect of Eu doping and partial oxygen isotope substitution on magnetic phase transitions in $(Pr_{1-y}Eu_y)_{0.7}Ca_{0.3}CoO_3$ cobaltites, J. Exp. Theor. Phys. 118 (2014) 266–278.
[16] I.A. Nekrasov, S.V. Sreltsov, M.A. Korotin, V.I. Anisimov, Influence of rare-earth ion radii on the low-spin to intermediate-spin state transition in lanthanide cobaltite perovskites: $LaCoO_3$ versus $HoCoO_3$, Phys. Rev. B 68 (2003) 235113 (1–7).
[17] K. Knizek, Z. Jirak, J. Hejtmanek, M. Veverka, M. Marysko, G. Maris, T.T.M. Palstra, Structural anomalies associated with the electronic and spin transitions in $LnCoO_3$, Eur. Phys. J. B 47 (2005) 213–220.
[18] V.G. Bhide, D.S. Rajoria, Y.S. Reddy, G. Rama Rao, G.V. Subba Rao, C.N.R. Rao, Localized-to-Itinerant electron transitions in rare-earth cobaltates, Phys. Rev. B 28 (1972) 1133–1136.
[19] S. Yamaguchi, Y. Okimoto, Y. Tokura, Bandwidth dependence of insulator-metal transitions in perovskite cobalt oxides, Phys. Rev. B 54 (1996) 11022–11025.
[20] (a) M. James, L. Morales, K. Wallwork, M. Avdeev, R. Withers, D. Goossens, Structure and magnetism in rare earth strontium-doped cobaltates, Phys. B 385–386 (2006) 199–201;
(b) M. James, T. Tedesco, D.J. Cassidy, R.L. Withers, oxygen vacancy ordering in strontium doped rare earth cobaltate perovskites $Ln_{1-x}Sr_xCoO_{3-\delta}$ (Ln = La, Pr and Nd; $x > 0.60$), Mater. Res. Bull. 40 (2005) 990–1000.
[21] S.N. Vereshchagin, L.A. Solov'yov, E.V. Rabchevskii, V.A. Dudnikov, S.G. Ovchinnikov, A.G. Anshits, Methane oxid at ion over A-site ordered and disordered $Sr_{0.8}Gd_{0.2}CoO_{3-\delta}$ perovskites, Chem. Commun. 50 (2014) 6112–6115.
[22] V.A. Dudnikov, Yu.S. Orlov, S.Yu Gavrilkin, M.V. Gorev, S.N. Vereshchagin, L.A. Solov'yov, N.S. Perov, S.G. Ovchinnikov, Effect of Gd and Sr ordering in A sites of doped $Gd_{0.2}Sr_{0.8}CoO_3-\delta$ perovskite on its structural, magnetic, and thermodynamic properties, J. Phys. Chem. 120 (2016) 13443–13449.
[23] S.N. Vereshchagin, V.A. Dudnikov, N.N. Shishkina, L.A. Solov'yov, Phase transformation behavior of $Sr_{0.8}Gd_{0.2}CoO_{3-\delta}$ perovskite in the vicinity of order-disorder transition, Thermochim. Acta 655 (2017) 34–41.
[24] V.A. Dudnikov, Yu.S. Orlov, N.V. Kazak, A.S. Fedorov, L.A. Solov'yov, S.N. Vereshchagin, A.T. Burkov, S.V. Novikov, S.Yu Gavrilkin, S.G. Ovchinnikov, Effect of A-site cation ordering on the thermoelectric properties of the complex cobalt oxides $Gd_{1-x}Sr_xCoO_{3-\delta}$ (x = 0.8 and 0.9), Ceram. Int. 44 (2018) 10299–10305.
[25] K. Conder, E. Pomjakushina, A. Soldatov, E. Mitberg, Oxygen content determination in perovskite-type cobaltates, Mater. Res. Bull. 40 (2005) 257–263.
[26] J.W. Visser, A. Fully, Automatic program for finding the unit cell from powder data, J. Appl. Crystallogr. 2 (1969) 89–95.
[27] H.M. Rietveld, A profile refinement method for nuclear and magnetic structures, J. Appl. Crystallogr. 2 (1969) 65–71.
[28] L.A. Solov'yov, Full-profile refinement by derivative difference minimization, J. Appl. Crystallogr. 37 (2004) 743–749.
[29] (a) A.T. Burkov, A. Heinrich, P.P. Konstantinov, T. Nakama, K. Yagasaki, Experimental set-up for thermopower and resistivity measurements at 100-1300 K, Meas. Sci. Technol. 12 (2001) 264–272;
(b) A.T. Burkov, A.I. Fedotov, A.A. Kasyanov, R.I. Panteleev, T. Nakama, Methods and technique of thermopower and electrical conductivity measurements of thermoelectric materials at high temperatures, Sci. Tech. J. Inf. Technol., Mech. Opt. 15 (2) (2015) 173–195.
[30] S.N. Vereshchagin, V.A. Dudnikov, L.A. Solov'yov, DSC + TG and XRD study of order-disorder transition in nonstoichiometric Sr-Gd-cobaltate, J. Sib. Fed. Univ. Chem. 3 (9) (2016) 326–336.
[31] R. Robert, M.H. Aguirre, L. Bocher, M. Trottmann, S. Heiroth, T. Lippert, M. Döbeli, A. Weidenkaff, Thermoelectric properties of $LaCo_{1-x}Ni_xO_3$ polycrystalline samples and epitaxial thin films, Solid State Sci. 10 (2008) 502–507.
[32] R. Robert, L. Bocher, M. Trottmann, A. Reller, A. Weidenkaff, Synthesis and high-temperature thermoelectric properties of Ni and Ti substituted $LaCoO_3$, J. Solid State Chem. 179 (2006) 3893–3899.
[33] S.G. Harizanova, E.N. Zhecheva, V.D. Valchev, M.G. Khristova, R.K. Stoyanova, Improving the thermoelectric efficiency of Co based ceramics, Mater. Today.: Proc. 2 (2015) 4256–4261.
[34] S. Behera, V.B. Kamble, S. Vitta, A.M. Umarji, C. Shivakumara, Synthesis structure and thermoelectric properties of La1-$x$$Na_xCoO_3$ perovskite oxides, Bull. Mater. Sci. 40 (7) (2017) 1291–1299.
[35] D. Moser, L. Karvonen, S. Populoh, M. Trottmann, A. Weidenkaff, Influence of the oxygen content on thermoelectric properties of $Ca_{3-x}Bi_xCo_4O_{9+\delta}$ system, Solid State Sci. 13 (2011) 2160–2164.